Fabrication and Electrical Characterization of Al/Ba$_x$Sr$_{1-x}$TiO$_3$/Pt/SiO$_2$/Si Configuration for FeFET Applications

Ala'eddin A. Saif, Z. A. Z. Jamal, Z. Sauli, P. Poopalan

Abstract—The ferroelectric behavior of barium strontium titanate (BST) in thin film form has been investigated in order to study the possibility of using BST for ferroelectric gate-field effect transistor (FeFET) for memory devices application. BST thin films have been fabricated as Al/BST/Pt/SiO$_2$/Si-gate configuration. The variation of the dielectric constant (ε) and tan δ with frequency have been studied to ensure the dielectric quality of the material. The results show that at low frequencies, ε increases as the Ba content increases, whereas at high frequencies, it shows the opposite variation, which is attributed to the dipole dynamics. tan δ shows low values with a peak at the mid-frequency range. The ferroelectric behavior of the Al/BST/Pt/SiO$_2$/Si has been investigated using C-V characteristics. The results show that the strength of the ferroelectric hysteresis loop increases as the Ba content increases; this is attributed to the grain size and dipole dynamics effect.

Keywords—BST thin film, Electrical properties, Ferroelectric hysteresis, Ferroelectric FET.

I. INTRODUCTION

FOR the past few years, ferroelectric random access memories (FRAMs) have attracted much attention due to their potential advantages such as nonvolatile, unlimited write cycles and low power consumption. In particular, nondestructive read out (NDRO) FRAM which has a transistor as a memory cell is attractive, since the ferroelectric gate offers simpler circuits and excellent performances [1], [2]. In general, there are two types of ferroelectric field effect transistors (FeFET); metal-ferroelectric-semiconductor (MFS) FET and Metal-ferroelectric-metal-insulator-semiconductor (MFMIS) FET. In fact, the latter consist of a ferroelectric capacitor and a conventional MOSFET. Due to the remnant polarization of the ferroelectric materials, the retained charges at the bottom electrode of the capacitor are coupled to the semiconductor and the conducting channel is then induced to allow the current flowing through drain to source.

Barium strontium titanate (Ba$_{1-x}$Sr$_x$TiO$_3$), or BST, in thin film form is considered one of the most leading candidates for ferroelectric field effect transistor (FeFET) application due to the desirable properties such as high permittivity and relatively high remnant polarization. BST is a solid solution family composed of barium titanate and strontium titanate with Curie temperature covering a wide range of temperature [3], [4]. In BST when strontium ions are introduced at A sites of the ABO$_3$ perovskite matrix, many parameters will be effected such as the unit cell volume and curie temperature [3], which in turn directly affects on the grain sizes and the lattice shape, i.e. cubic or tetragonal structure, of BST. In addition, the grain size of the thin films has a significant effect on the ferroelectric properties, such as remnant polarization and coercive field [5].

Few studies have been focused on characterizing BST for FeFET applications. In a previous work, we studied the memory window behavior of BST in MIS configuration [6]. However, this work will present BST thin films in MFMIS structure to study the possibility of using BST for FeFET applications.

II. EXPERIMENT

Three solutions with proportions of Ba:Sr (50:50, 70:30 and 80:20) were prepared using barium acetate, strontium acetate and titanium (IV) isopropoxide as the starting material, the preparation details for the solution can be found somewhere else [7], [8]. The prepared solutions were consecutively named BST50, BST70 and BST80. These solutions were deposited on the Pt/SiO$_2$/Si substrate, using the film fabrication procedures reported in [7] and [8]. In order to measure the films thickness, the films were partially dipped in a diluted hydrofluoric acid (HF); the resulting step-profile thickness was measured with a stylus profilometer. The average thickness of the prepared films is measured to be 450 nm. The crystallization of the films has been determined using an X-Ray diffractometer (XRD) with a CuKα radiation source (λ = 1.54 Å), and operated at a voltage of 40 KV and a current of 40 mA. For the electrical measurement, dots of Al with an area of 7.85×10^{-3} cm^2 were deposited on top of the films through a shadow mask using a physical vapor deposition (PVD) technique to represent the top electrode. Thus, the electrical measurements were carried out on Al/BST/Pt/SiO$_2$/Si (MFMIS) structures. The dielectric characteristics were performed by an impedance/gain-phase analyzer (Solartron 1260) in the frequency range of 10 Hz to 1 MHz at room temperature. The capacitance-voltage (C-V) and the current-voltage (I-V) curves were measured using Keithley 4200 semiconductor parameter analyzer.

III. RESULTS AND DISCUSSION

A. XRD Analysis

Fig. 1 shows the X-ray diffraction patterns of BST50, BST70 and BST80 films. It can be observed from the figure

Microfabrication Cleanroom, School of Microelectronic Engineering, University Malaysia Perlis, Kuala Perlis, 02000 Perlis, Malaysia
Corresponding author: +60 19 4948919, alasaif82@hotmail.com
(Ala'eddin A. Saif)

World Academy of Science, Engineering and Technology
International Journal of Materials and Metallurgical Engineering
Vol:5, No:9, 2011

that the diffraction peaks are (1 0 0), (1 1 0), (1 1 1), (2 0 0), (2 1 0) and (2 1 1) within the 2θ range from 20° to 60°, which confirms that the films are crystallized with the Perovskite structure. The measured lattice parameters of the samples are listed in Table 1. It is observed that the lattice parameters decrease with the increasing strontium content. This decrease can be explained according to the fact that as Sr^{2+} ions are introduced at the A site of the Perovskite matrix, they enter substitutionally on the Ba^{2+} site; consequently, as the Sr content increases, a small decrease in the unit cell volume takes place [8]. Table 1 shows that the lattice constants for BST50 are equal, which reveals that it has a simple cubic structure, whereas, for BST70 and BST80 films, the c-axis lattice constant is larger than the a-axis lattice constant. This suggests that the crystal structure for these films is tetragonal at room temperature.
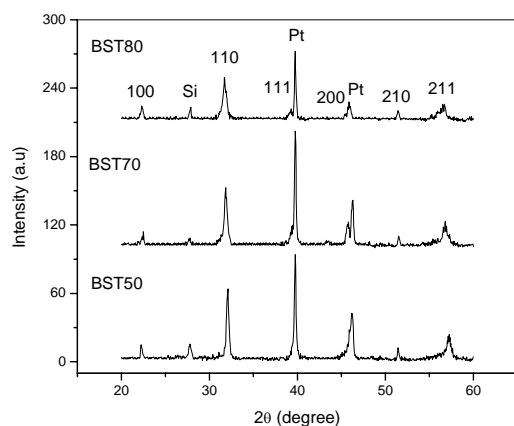

Fig. 1 XRD patterns for BST50, BST70 and BST80 thin films

TABLE I
LATTICE PARAMETERS OF BST50, BST70 AND BST80 FILMS

Sample	a (Å)	c (Å)	c/a	Structure phase
BST50	3.9471	3.9471	1	Simple cubic
BST70	3.9771	3.9883	1.003	Tetragonal
BST80	3.9785	4.0173	1.0098	Tetragonal

B. Electric and Ferroelectric Characteristics

Fig. 2 shows the variation of ε with frequency plots for the films used in this work at room temperature. It is observed that the value of ε for all film decreases as the frequency increases and attains a constant limiting value ε_∞ (high-frequency value of ε). This can be explained according to the behavior of the dipoles movement, the dielectric permittivity related to free dipoles oscillating in the presence of an alternating electric field. At very low frequencies ($f < 1/\tau$, τ is the relaxation time), dipoles follow the electric field. As the frequency increases, dipoles begin to lag behind the field and ε slightly decreases. When the frequency reaches the characteristic frequency ($f = 1/\tau$), the dielectric constant drops (relaxation process). At very high frequencies ($f > 1/\tau$), dipoles can no longer follow the field and $\varepsilon \approx \varepsilon_\infty$ [9].

From Fig. 2, it can be seen that at low frequencies, the value of ε increases as the Ba content increases. This can be explained according to the lattice shape and the presence of the dipoles in the BST lattice. It is discussed earlier in this article that BST70 and BST80 films are crystallized in a tetragonal phase which leads that their lattice contains a valuable number of permanent diploes whereas BST50 lacks to this kind of dipoles since it is crystallize with a cubic phase. That explains the high value of dielectric constant for BST70 and BST80 films compared to BST50. Furthermore, the high value of ε for BST80 compared to BST70 can be attributed to the longer permanent dipoles, since the c/a ratio for BST80 is larger than that for BST70.
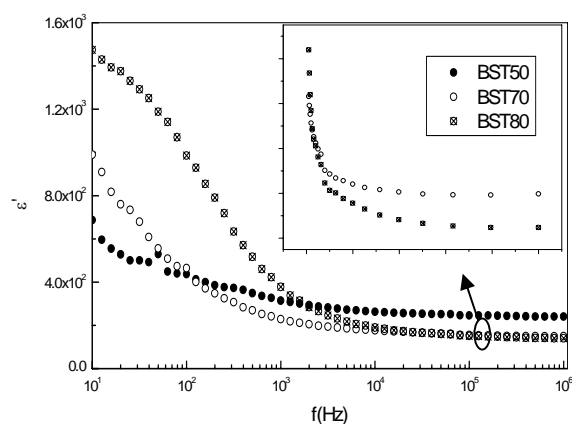

Fig. 2 Variation of ε with frequency for various Ba:Sr ratio at room temperature.

On the other hand, at high frequencies, the dielectric constant variation with Ba content becomes the opposite of that observed at low frequencies; i.e. ε decreases as the Ba content increases. This may be explained considering the dipole elongation responding to the applied electric field. As an AC electric field is applied at BST lattice, it creates a new dipoles, reorients the permanent dipoles to the direction of the applied field and causes an induced shift to the Ti ions for the dipoles that are already have the same orientation of the applied field in case of BST70 and BST80 films, which in turn increases their length. However, as the frequency increases, the longer dipoles find it harder to follow the applied field, as a result, a low dielectric constant is obtained. Furthermore, the trend of ε at high frequencies agrees very well with the published results in the literature [3]. The value of ε in the whole frequency range is relatively high.

The variation of tan δ as a function of frequency is given in Fig. 3. It can be observed from the figure that at low frequencies tan δ decreases with increasing frequency and reaches a value close to zero at high frequencies. At a frequency range between 250 to 10^5 Hz, a broad peak in BST70 and BST80 is observed. This kind of peak occurs when the hopping frequency of electric charge carriers

World Academy of Science, Engineering and Technology
International Journal of Materials and Metallurgical Engineering
Vol:5, No:9, 2011

approximately equal to that of the external applied AC electric field [10], however, this peak becomes more noticeable and shifts toward lower frequencies as the Ba content increases. This could be attributed to the increase of the grain sizes and dipoles present. From the above results it can be concluded that the dielectric properties of the films used in this work are relatively good.
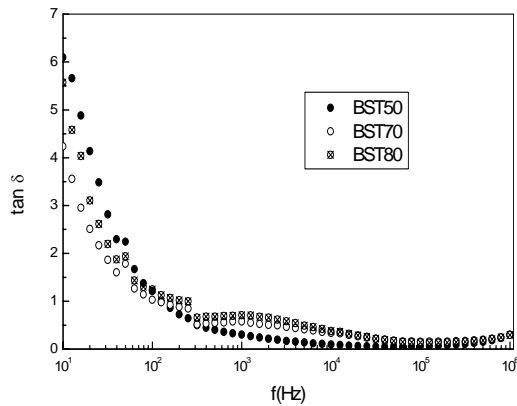

Fig. 3 Variation of tan δ versus frequency for various Ba:Sr ratios at room temperature.

The ferroelectric properties for the films used in this work were performed using the capacitance-voltage (C-V) characteristics technique. Fig. 4 shows the C-V characteristics for BST50, BST70 and BST80 at 500 KHz and at room temperature. The capacitance was measured while a DC field was swept from -7.5 to +7.5 V and then reversed, with a sweeping rate of 0.01 V/s. For all the tested samples, it is observed that the capacitance varies non-linearly with the applied voltage. However, a well-defined butterfly shape with two peaks of the capacitance is observed, these peaks are formed as a result of a spontaneous polarization switching. This kind of hysteresis indicates that these films have a ferroelectric nature. However, the hysteresis loop for the current samples resembles to the memory window for MFIS configuration.
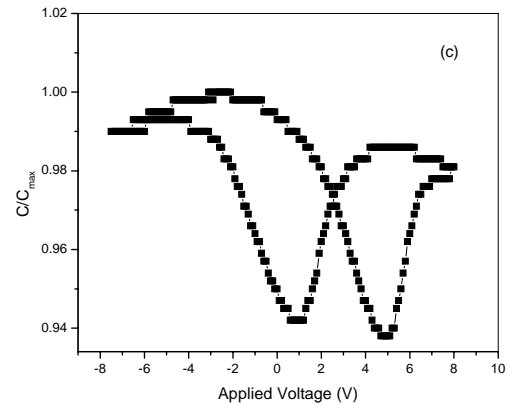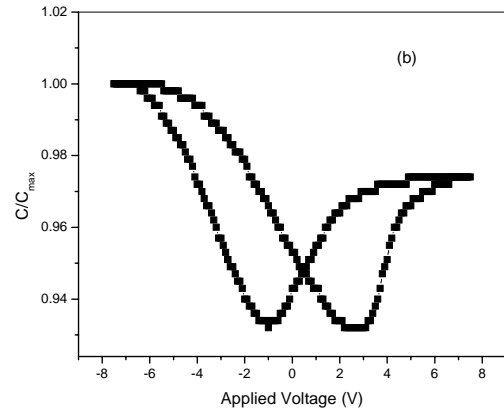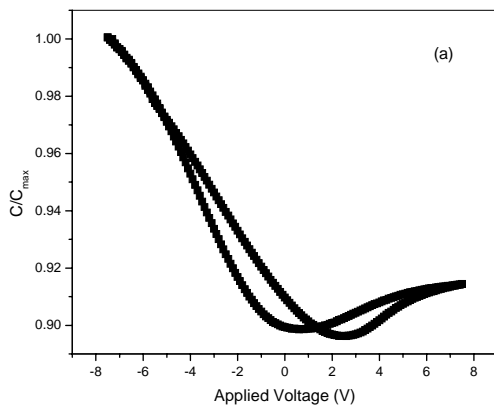

(c)

Fig. 4 C-V characteristics for (a) BST50, (b) BST70 and (c) BST80 thin films within the MFMIS configuration.

It can be observed from the figure that the hysteresis loop strength increases as the Ba content increases. This increment is attributed to the permanent dipoles present and grain size effects. XRD analysis reveals that BST70 and BST80 films crystallize with a tetragonal structure while BST50 crystallized with a cubic structure, which leads to the valuable number of permanent dipoles that exist within the Perovskite lattice of BST70 and BST80; these dipoles contribute to the ferroelectric behavior subsequently at the hysteresis loop strength. On the other hand, the increment of the hysteresis loop strength can be explained based on the grain size effect. It has been found in previous work that the grain size of BST increases with the increasing of the Ba content [8]. However, it is mentioned earlier in this article that the ferroelectric properties, such as remnant polarization and coercive field, strongly depend on the grain size. In addition, G. Arlt *et al.* presented theoretical calculations showing that the density of the domain walls is inversely proportional to the square root of the grain size [11], i.e., the density of the domain walls increases as the grain size decreases. This in turn strengthens

World Academy of Science, Engineering and Technology
International Journal of Materials and Metallurgical Engineering
Vol:5, No:9, 2011

the repulsive force between neighboring domain walls. As a result, the mobility for the domain wall reduces, which in turn makes the domain reorientation more difficult [12]. Leading up to higher activation energy is required for the reorientation of the domains; as a result, the remnant polarization decreases, which in turn reflects as a strong hysteresis loop in C-V curves.

Furthermore, an observed asymmetry in the C–V curves suggests that the films contain mobile ions or charges accumulated at the interface between the film and the electrode. In addition, there is a difference between the capacitance values of the two peaks, which may be due to some defect in energy levels in the films [13].

A typical variation of leakage current density as a function of applied voltage (J-V) for the films used in this work, at room temperature, and for positive voltage swept from zero up to 8 V is shown in Fig. 5. It is observed that the leakage current density increases with the increase of the applied voltage, and it is found that for all the tested samples the leakage current density is of the order of 10^{-7} A/cm^2 at an applied voltage of 8 V (0.2 MV/cm). These values of the current density are relatively low, leading to good interface situations. Furthermore, it is observed that the leakage current density decreases as the Ba content decreases, which is attributed to the decrease of the grain size. It is well-known that the grain boundaries act as trappers for crystal defects (vacancies and dislocations) that interact with free carriers. Furthermore, as the grain size decreases the density of the grain boundaries increase, which leads to larger amount of vacancies and dislocations, giving rise to high density local charge accumulation. Those charge centers near the grain boundaries act to block the current flow, leading to low leakage current.
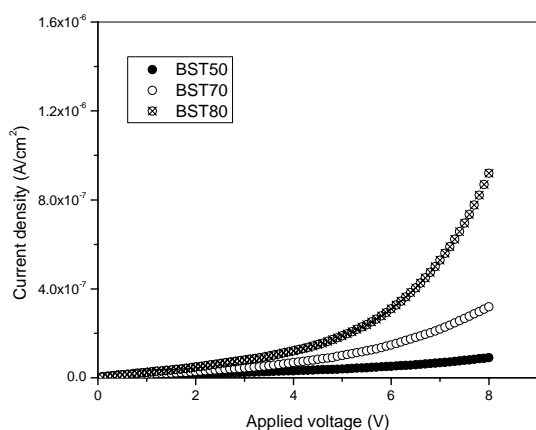

Fig. 5 Leakage current density for various Ba:Sr ratios at room temperature.

IV. CONCLUSION

Perovskit-type BST thin films have been successfully fabricated as MFMIS configuration. The quality of the films

has been confirmed via investigation the variation of the dielectric constant (ε) and tan δ as a function of frequency. The results show that at low frequencies, ε increases as the Ba content increases, whereas at high frequencies, it shows the opposite variation, which is attributed to the dipole dynamics. tan δ shows low values with a peak at the mid-frequency range. The ferroelectric behavior of the films has been investigated using C-V characteristics. The results show that the strength of the ferroelectric hysteresis increases as the Ba content increases; this is attributed to the grain size and dipole dynamics effect. The formation of the hysteresis loop for the films in the current work leads that BST in thin film form can be used for ferroelectric field effect transistor applications.

REFERENCES

[1] A. Roy, A. Dhar, D. Bhattacharya, S. K Ray, "Structural and electrical properties of metal–ferroelectric–insulator–semiconductor structure of Al/SrBi$_2$Ta$_2$O$_9$/HfO$_2$/Si using HfO$_2$ buffer," J. Phys. D: Appl. Phys., vol. 41, pp. 095408, 2008.

[2] Y. P. Wang, L. Zhou, X. B. Lu, Z. G. Liu, "C–V characteristics of Pt/PbZr$_{0.53}$Ti$_{0.47}$O$_3$/LaAlO$_3$/Si and Pt/PbZr$_{0.53}$Ti$_{0.47}$O$_3$/La$_{0.85}$Sr$_{0.15}$CoO$_3$/LaAlO$_3$/Si structures for ferroelectric gate FET memory," App. Surf. Sci., vol. 205, pp. 176-181, 2003.

[3] D. R. Patil, , S. A. Lokare, R. S. Devan, S. S. Chougule, C. M. Kanamadi, Y. D. Kolekar, B. K. Chougule, "Studies on Electrical and Dielectric Properties of Ba$_{1−x}$Sr$_x$TiO$_3$," Mater. Chem. Phys., Vol. 104, pp. 254-257, 2007.

[4] E. Ngo, W. D. Nothwang, C. Hubbard, S. Hirsch, M. W. Cole, W. Chang, S. W. Kirchoffer, J. M. Pond, "Ba$_{1-x}$Sr$_x$TiO3 ased Thin Films for Next Generation Devices," Army Research Laboratory 2004: Report Number: ARL-TN-228, Aberdeen Proving Ground, MD 21005-5069.

[5] S. K. Pandey, A. R. James, C. Prakash, T. C. Goel, K. Zimik, "Electrical properties of PZT thin films grown by sol-gel and PLD using a seed layer," Mater. Sci. Eng. B, vol. 112, pp. 96-100, 2004.

[6] Ala'eddin A. Saif, P. Poopalan, "Electrical properties of metal–ferroelectric–insulator–semiconductor structure using Ba$_x$Sr$_{1-x}$TiO$_3$ for ferroelectric–gate field effect transistor," Solid State Electron, vol. 62, pp. 25-30, 2011.

[7] Ala'eddin A. Saif, P. Poopalan, Effect of the Film Thickness on the Impedance Behavior of Sol-gel Ba$_{0.6}$Sr$_{0.4}$TiO$_3$ Thin Films," Physica b condensed matter, vol. 406, pp. 1283-1288, 2011.

[8] Ala'eddin A. Saif, P. Poopalan, "Impedance/Modulus Analysis of Sol-gel Ba$_x$Sr$_{1-x}$TiO$_3$ Thin Films," J. Korean Phys. Soc. vol. 57, pp. 1449-1455, 2010.

[9] R. Tripathi, A. Kumar, Ch. Bharti, T. P. Sinh, "Dielectric relaxation of ZnO nanostructure synthesized by soft chemical method', Curr. App. Phys., vol. 10, pp. 676-681, 2010.

[10] M. A. Elkestawy, S. Abdelkader, M. A. Amer, "AC conductivity and dielectric properties of Ti-doped CoCr$_{1.2}$Fe$_{0.8}$O$_4$ spinel ferrite," Physica B, vol. 405, pp. 619-624, 2010.

[11] G. Arlt, D. Hennings, G. De With, "Dielectric properties of fine‐grained barium titanate ceramics," J. Appl. Phys., vol. 58, pp. 1619-1625, 1985.

[12] S. H. Hu, G. J. Hu, X. J. Meng, G. S. Wang, J. L. Sun, S. L. Guo, J. H. Chu, N. Dai, "The Grain Size Effect of the Pb(Zr0.45Ti0.55)O3 Thin Films Deposited on LaNiO Coated Silicon by Modified Sol-gel Process," J. Cryst. Growth, vol. 260, pp. 109-114, 2004.

[13] N. Kumari, S. B. Krupanidhi, K. B. R. Varma, "Dielectric, impedance and ferroelectric characteristics of c-oriented bismuth vanadate films grown by pulsed laser deposition" Mat. Sci. Eng. B, vol. 138, pp. 22-30, 2007.